

expected value of ^{209}Bi α -decay, $Q_\alpha = 3,137 \pm 0.9$ keV (ref. 1, see comment in Supplementary Information).

Finally, possible contaminations by already-known α emitters of close Q_α were considered: ^{186}Os ($T_{1/2} = 2.0 \times 10^{15}$ years; $Q_\alpha = 2,822$ keV) and ^{190}Pt ($T_{1/2} = 6.5 \times 10^{11}$ years; $Q_\alpha = 3,249$ keV) were discarded because the results implied very high atomic concentrations, respectively Os/Bi $\approx 6,500$ p.p.m. and Pt/Bi ≈ 250 p.p.m. A dedicated quantitative Pt implantation experiment in BGO, followed by a secondary ion mass spectrometry (SIMS) analysis, proved that Pt concentration was under 2 p.p.m. Higher concentrations were very unlikely¹⁸, and would have strongly affected the scintillating properties of the crystal¹⁹.

The auxiliary observation of ^{209}Bi decay to the first excited state of ^{205}Tl (Fig. 1b) would constitute a conclusive test of our proper identification of the α line. Such a—negative—search was performed recently, using a very low background facility under the Oroville dam, where 204 keV γ -particles emerging from 1.8 kg of Bi_2O_3 were looked for²⁰. Thanks to the high Z of Bi, and to their slow time constant ($\tau \approx$ a few ms $\gg 1.5$ ns), BGO bolometers naturally sum the energies of the α -particle and of the following absorbed γ , adding another event to the ‘full energy’ peak. However, the γ escape probability is not negligible: we estimate it to be 12.8% in our 46-g BGO detector by Monte Carlo simulations. Taking into account internal conversion²¹, the overall efficiency for detecting α -decay at this level through recording of the escape peak is $\eta = 8.8\%$. With reasonable assumptions (see Supplementary Information), the associated partial half-life is estimated to be $T_{1/2} = 6\text{--}13 \times 10^{20}$ years: a two-month exposure would then probably lead to its detection (Table 1).

These data extend by more than three orders in magnitude the range of α -particle decays ever reported ($T_{1/2} = 7 \times 10^{15}$ years; ^{148}Sm). α -particle events may now be accurately tracked down to 500 keV, with background suppression efficiency over 98%, in common laboratory radioactive environments. Equivalent rejection power against γ -particles should be observed down to around 50 keV, provided that the confusing recoils background is reduced (in underground experiments, for example; see Supplementary Information). These possibilities in the search for rare events—indicated also by our recent improvements of the ^{180}W α -particle decay rate limit²²—justify the greater complexity added by the low-temperature requirements.

With this ^{209}Bi decay detection, BGO bolometers open up the rarest of natural main energy lines—whereas much rarer double β -particle decays are observed among naturally abundant elements²³, no line corresponding to the neutrinoless mode $0\nu\beta\beta$ has been hitherto convincingly reported. This particular property motivated recent searches for ^{209}Bi decay: with respect to the search for proton decay, a proposal was made to use ‘freshly produced’ bismuth to check for deviation of radioactive decay from the exponential law at small times^{24,25}. □

Received 20 November 2002; accepted 10 March 2003; doi:10.1038/nature01541.

- Audi, G., Bersillon, O., Blachot, J. & Wapstra, A. H. The Nubase evaluation of nuclear and decay properties. *Nucl. Phys. A* **624**, 1–124 (1997).
- Hincks, E. P., Millar, C. H. & Hanna, G. C. A search for α -particles from the decay of ^{209}Bi . *Can. J. Phys.* **36**, 231–251 (1958).
- de Carvalho, H. G. & de Araújo Penna, M. Alpha-activity of ^{209}Bi . *Lett. Nuovo Cim.* **3**, 720–722 (1972).
- Jenkner, K. & Broda, E. Some upper limits of possible alpha-activity. *Nature* **164**, 412–413 (1949).
- Faraggi, H. & Berthelot, A. Sur la radioactivité alpha du bismuth naturel. *C. R. Acad. Sci.* **232**, 2093–2095 (1951).
- Riezler, W. & Porschen, W. Natürliche Radioaktivität von Wismut. *Z. Naturforsch.* **7a**, 634–635 (1952).
- Gonzalez-Mestres, L. & Perret-Gallix, D. Detection of low energy solar neutrinos and galactic dark matter with crystal scintillators. *Nucl. Instrum. Meth. A* **279**, 382–387 (1989).
- Bobin, C. *et al.* Alpha/gamma discrimination with a $\text{CaF}_2(\text{Eu})$ target bolometer optically coupled to a composite infrared bolometer. *Nucl. Instrum. Meth. A* **386**, 453–457 (1997).
- Alessandrello, A. *et al.* Development of a thermal scintillating detector for double beta decay of ^{48}Ca . *Nucl. Phys. B (Proc. Suppl.)* **28A**, 233–235 (1992).
- Moses, W. W. *et al.* Prospects for dense, infrared emitting scintillators. *IEEE Trans. Nucl. Sci.* **45** (3), 462–466 (1998).
- Ziegler, J. F. *The Stopping and Ranges of Ions in Matter* Vol. 4, *Helium: Stopping Powers and Ranges in All Elemental Matter* (Pergamon, New York, 1977).

- Coron, N. *et al.* A composite bolometer as a charged-particle spectrometer. *Nature* **314**, 75–76 (1985).
- Cebrián, S. *et al.* The ROSEBUD experiment at Canfranc: 2001 report. *Nucl. Phys. B (Proc. Suppl.)* **110**, 97–99 (2002).
- Zhou, J. W. *et al.* Advances towards fast thermal detectors of intermediate mass with high resolution and large dynamic range. *Nucl. Instrum. Meth. A* **335**, 443–452 (1993).
- Alessandrello, A. *et al.* Preliminary results on the performance of a TeO_2 thermal detector in a search for direct interactions of WIMPs. *Phys. Lett. B* **384**, 316–322 (1996).
- Rasmussen, J. O. Alpha-decay barrier penetrabilities with an exponential nuclear potential: even-even nuclei. *Phys. Rev.* **113**, 1593–1598 (1959).
- Rasmussen, J. O. Alpha-decay barrier penetrabilities with an exponential nuclear potential: odd-mass nuclei. *Phys. Rev.* **115**, 1675–1679 (1959).
- Zhou, T. Q., Tan, H. R., He, C. F., Zhu, R. Y. & Newman, H. B. Determination of trace elements in BGO by neutron activation analysis. *Nucl. Instrum. Meth. A* **258**, 58–66 (1987).
- Barnes, R. G. L., Sims, R., Rousseau, M. D. & Sproston, M. Bismuth germanate (BGO) optimisation for energy resolution and purity. *IEEE Trans. Nucl. Sci.* **31**, 249–252 (1984).
- Norman, E. B. *et al.* Diamonds, maybe, but bismuth is not forever. *Bull. Am. Phys. Soc.* **45**, 30 (2000).
- Giannatiempo, A. & Perego, A. Penetration effects in the internal conversion process of the 204 KeV transition in ^{205}Tl . *Z. Phys. A* **308**, 247–251 (1982).
- Cebrián, S. *et al.* Improved limits for natural α radioactivity of tungsten with a CaWO_4 scintillating bolometer. *Phys. Lett. B* **556**, 14–20 (2003).
- Tretyak, V. I. & Zdesenko, Y. G. Tables of double beta decay data—an update. *Atom. Data Nucl. Data Tables* **80**, 83–116 (2002).
- DeBraeckeleer, L. *et al.* Measurement of lifetime of ^{209}Bi and test of the exponential decay law. *TUNL Progr. Rep.* **37**, 94 (1998).
- DeBraeckeleer, L., Gould, C. R. & Tornow, W. Search for $T_{1/2}$ of the “stable” nucleus ^{209}Bi . *TUNL Progr. Rep.* **38**, 87–89 (1999).
- Powell, C. F., Fowler, P. H. & Perkins, D. H. *The Study of Elementary Particles by the Photographic Method. An Account of the Principal Techniques and Discoveries Illustrated by an Atlas of Photomicrographs* 137–138, 644–645 (Pergamon, New York, 1959).
- Firestone, R. B. *Table of Isotopes*, 8th edn, Vol. II: A = 151–272 (eds Shirley, V. S., Baglin, C. M., Chu, S. Y. F. & Zipkin, J.) 2545, 2595 (Wiley, New York, 1996).

Supplementary Information accompanies the paper on Nature’s website (<http://www.nature.com/nature>).

Acknowledgements This work is supported by the R&D programme from CNRS/INSU, and by BNM for the high-resolution α -spectrometry part. The design of the optical detectors results from years of support by CNES. P. Pari from CEA/SPEC designed our dilution refrigerator. We thank the SEMIRAMIS members of CSNSM for their accurate implantation, as well as F. Jomard for SIMS analysis, G. Audi for discussions, E. Leblanc from LNH/BNM for independent calibration source measurements, and I. Rameau and Y. Bouvry for their support and comments.

Competing interests statement The authors declare that they have no competing financial interests.

Correspondence and requests for material should be addressed to P.d.M. (e-mail: pierre.demarcillac@ias.u-psud.fr) or N.C. (e-mail: noel.coron@ias.u-psud.fr).

Magmatic events can produce rapid changes in hydrothermal vent chemistry

Marvin D. Lilley*, David A. Butterfield†, John E. Lupton‡ & Eric J. Olson*

* School of Oceanography, University of Washington, Seattle, Washington 98195-5351, USA

† Joint Institute for the Study of the Atmosphere and Ocean, University of Washington, and Pacific Marine Environmental Laboratory, NOAA, Seattle, Washington 98195, USA

‡ Pacific Marine Environmental Laboratory, NOAA, Newport, Oregon 97365, USA

The Endeavour segment of the Juan de Fuca ridge is host to one of the most vigorous hydrothermal areas found on the global mid-ocean-ridge system, with five separate vent fields located within 15 km along the top of the ridge segment¹. Over the past decade, the largest of these vent fields², the ‘Main Endeavour Field’, has exhibited a constant spatial gradient in temperature and chloride concentration in its vent fluids, apparently driven by differences in the nature and extent of subsurface phase separation³. This stable situation was disturbed on 8 June 1999 by an earthquake

swarm⁴. Owing to the nature of the seismic signals and the lack of new lava flows observed in the area during subsequent dives of the *Alvin* and *Jason* submersibles (August–September 1999), the event was interpreted to be tectonic in nature⁴. Here we show that chemical data from hydrothermal fluid samples collected in September 1999 and June 2000 strongly suggest that the event was instead volcanic in origin. Volatile data from this event and an earlier one at 9° N on the East Pacific Rise show that such magmatic events can have profound and rapid effects on fluid–mineral equilibria, phase separation, ³He/heat ratios and fluxes of volatiles from submarine hydrothermal systems.

There is no evidence of recent volcanism in the area of the Main Endeavour Field (MEF; Supplementary Fig. 1), and a 0.5-km-wide axial valley indicates that the area is currently in a tectonically controlled phase⁵. In 1988, a weak seismic reflector was imaged at about 2.5 km depth⁶, but a later refraction experiment showed no evidence for a low-seismic-velocity zone (magma chamber) beneath this reflector⁷. Recent seismic data indicate that on-axis micro-earthquakes persist to a depth of 3.5 km below the sea floor, well below the weak seismic reflector at 2.5 km, although most occur above 3 km (ref. 8). For these reasons, Endeavour has become the type example for a ‘cracking front’ hydrothermal system, in which heated sea water continually penetrates deeper within a frozen magma chamber and extracts heat from the gabbroic layer^{9,10}. However, new seismic reflection data collected in July 2002 indicate a magma body at about 2.3–2.6 km depth¹¹. This forces us to re-examine our ideas about the heat source driving the Endeavour hydrothermal system, and to consider whether periodic magma resupply¹² may be important.

Although the earthquake swarm was originally argued to be a tectonic event⁴, a reanalysis of the seismic data has shown it to be more consistent with a volcanic event¹³. Additionally, perturbations in crustal fluid pressure and temperature recorded at Ocean Drilling Program (ODP) sites on the eastern flank of the Endeavour segment indicated that the seismic energy generated by the earthquake swarm could account for only a small fraction of the estimated 12 cm displacement¹⁴. Thus, most of the displacement was aseismic, and occurred slowly enough not to produce seismic waves. This is consistent with slow magma movement.

CO₂ and He are magmatic volatiles that are strongly enriched in areas with active magma chambers, such as Axial volcano¹⁵, Loihi seamount¹⁶ and the eruptive area at 9° 50′ N on the East Pacific Rise^{17,18} (EPR). The concentrations of these two volatiles were relatively stable in fluids from five selected sulphide edifices (Hulk, Dante, Bastille, Puffer and Sully) in the MEF during the period 1991–98. However, in 1999 their concentrations dramatically increased and then declined to near pre-event values in 2000 (Fig. 1a, b; Supplementary Table 1). If we assume that the high-temperature reaction zone beneath Endeavour is about 2.5 km below the sea floor¹¹, the basaltic saturation value for CO₂ at this depth is 5 mmol kg⁻¹ (ref. 19). Field data from the Juan de Fuca ridge indicate that CO₂ concentrations in most basalts range from saturation to twice saturation²⁰. On the basis of Li/Cl ratios, the water/rock ratio before and after the 1999 event remains relatively unchanged, and is about 2 (refs 3, 21; Fig. 1c; Supplementary Table 1). Assuming CO₂ values twice saturation, and allowing for the complete extraction of CO₂ in a single-pass system, rock extraction can only account for a fluid concentration of 5 mmol kg⁻¹. A tectonic event exposing new rock will not increase the CO₂ concentration without a reduction in the water/rock ratio. Water/rock ratios approaching 0.1 would be required to achieve the high CO₂ concentrations measured in 1999. As such low values were not seen, a magmatic source is required for the increased CO₂.

The significant drop in Cl concentration at Sully and Puffer immediately following the 1999 event (Fig. 1d) could be caused by increased phase separation induced by heat from either a tectonic or magmatic event. However, phase separation alone cannot explain the changes in gas concentration. Before 1999, these sulphide structures already exhibited low Cl concentrations owing to continuing phase separation. Increased phase separation should further increase the concentrations of gases, but this did not happen for all gases. For example, there was only a small increase in N₂ and Ar concentrations in 1999 beyond that seen in previous years (data not shown), whereas there was a 5-fold increase in CO₂ at Puffer in 1999 relative to 1998 (Fig. 1a). N₂ and Ar in vent fluids are primarily derived from circulating sea water and, except for a small Ar contribution from the mantle²², behave conservatively in the hydrothermal circulation cell. The relatively unchanged values for N₂ and

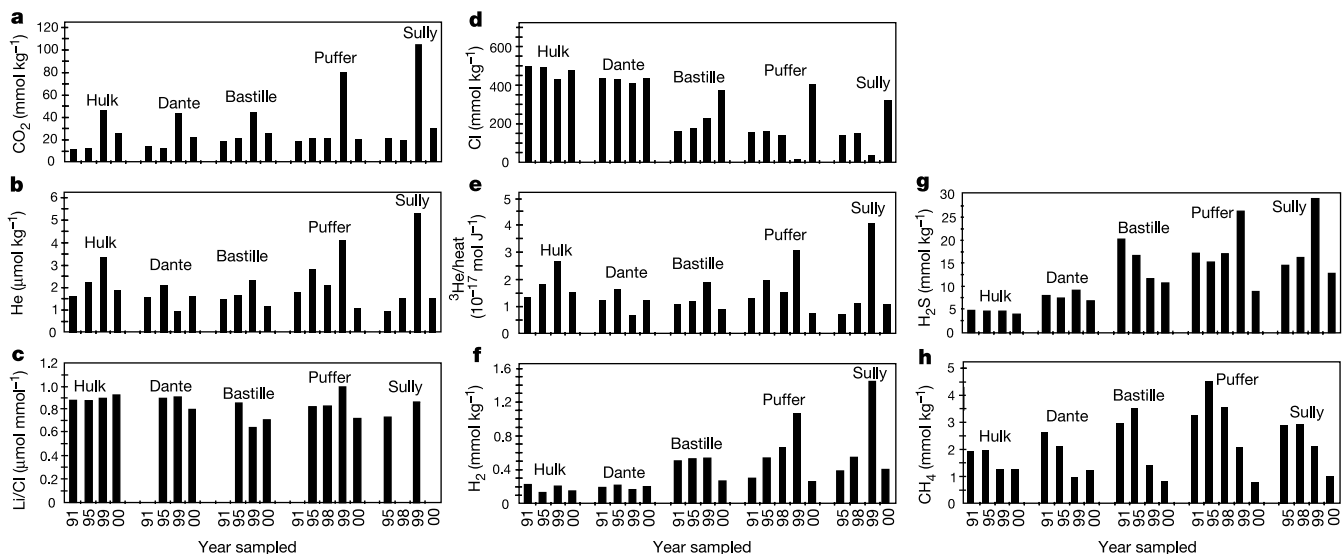


Figure 1 Time-series data for five of the major sulphide structures within the MEF. Shown are the concentrations of CO₂ (a), He (b), Cl (d), H₂ (f), H₂S (g) and CH₄ (h); also shown are the ratios Li/Cl (c) and ³He/heat (e). The values are ‘endmember’ concentrations. During sampling, small amounts of ambient sea water are entrained. This effect is removed by extrapolating to zero Mg concentration, as pure hydrothermal fluid contains

no Mg. The earthquake swarm started on 8 June 1999. The 1999 fluid samples were collected in September with DSV *Alvin* using gas-tight titanium samplers. The gases were extracted under vacuum at sea, and sealed in break-seal glass ampoules for analysis on shore by gas chromatography.

Ar indicate that the increased degree of phase separation in 1999 does not account for the large increases in CO₂ and He at Sully and Puffer (Fig. 1a, b). A shift to supercritical phase separation (brine condensation) at depth²³ could reduce the Cl content of the vapour phase without significantly altering the gas content. This, coupled with the earlier discussion of CO₂ extraction from basalt, indicates input from a magmatic source.

Before 1999, both Sully and Puffer had Cl concentrations (135–160 mmol kg⁻¹) much below that of sea water (540 mmol kg⁻¹). These low Cl values are indicative of a stable phase separation condition before the 1999 event. In 1999, however, the Cl concentration in MEF fluids decreased at four of the five sites, most dramatically at Puffer and Sully (Fig. 1d). In contrast, the Cl concentration at Bastille (near Puffer and Sully) increased in 1999, indicating the complexity of the effect of the event on the nature and degree of phase separation. In 2000, the Cl concentrations measured at Puffer, Sully and Bastille were more than double their respective concentrations seen before the event. Similar behaviour in Cl concentration after a magmatic event was seen at 'A' vent in 1991 on the EPR²⁴. Conversely, an apparent tectonic event on the EPR in 1995 had relatively little effect on Cl concentrations at nearby vents²⁵.

Without a decrease in water/rock ratio, elevated ³He/heat ratios can also be taken to be a clear indicator of recent perturbation by magmatic activity. In all instances where data are available, the ³He/heat ratio of fluids sampled after sea-floor volcanic events has been found to be elevated above the mean value of 0.5 × 10⁻¹⁷ mol J⁻¹ for 'mature' hydrothermal fluids and to decline with time after the event²⁶. At MEE, the ³He/heat ratio increased significantly at four of the five structures studied after the 1999 event, and then decreased back to, or below, the values recorded in preceding years (Fig. 1e). Our measurements at Endeavour were made approximately 4 months after the seismic event, and again at 1 year after the event. The relatively rapid decrease of CO₂ and He concentrations and ³He/heat ratio back to pre-event levels within one year is similar to that observed at the 'A' vent at 9° 46.5' N on the EPR. At 'A' vent, the rapidly changing volatile concentrations (Fig. 2) were associated with the emplacement of a dyke about 200 m below the sea floor just two weeks before the collection of the first samples²². The rapid decrease in ³He/heat ratio and corresponding increase in CO₂ concentrations indicates that CO₂ and He were differentially released during this magmatic event. These are the only volatile data documenting the early stages of such an event. By 1992, the 'A' vent ³He/heat ratio had decreased to values similar to that at Endeavour. Concomitant initial decreases in Cl

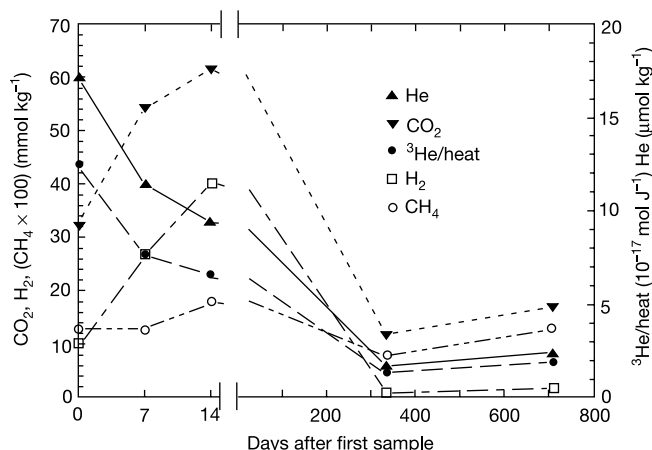


Figure 2 Time-series data for 'A' vent at 9° N on the EPR. Shown are concentrations of He, CO₂, H₂ and CH₄, and the ³He/heat ratio. Samples were collected with DSV *Alvin* on 10, 17 and 24 April 1991; 10 March 1992; and 26 March 1994.

concentration and increases in H₂S were also noted at 'A' vent²².

In addition to an increase in CO₂ and He concentrations, the 1999 Endeavour event resulted in significant increases in H₂ and H₂S concentrations in some of the vents (Fig. 1f, g). Similar enrichments were noted at 'A' vent immediately following the dyke injection on the EPR, where H₂ values are the highest measured in hydrothermal fluids (Fig. 2). The concentration of H₂ in hydrothermal fluids is controlled by pressure, temperature, Cl concentration, and fluid–mineral equilibria²⁷. For a reaction zone at 400 °C and 500 bar, a mineral assemblage consisting of anhydrite + anorthite, clinozosite, pyrite and magnetite would result in an H₂ concentration of about 0.2 mmol kg⁻¹ (ref. 27). This fits well with the H₂ concentrations seen at Hulk and Dante (Fig. 1f). H₂ concentrations of the order of 0.5 mmol kg⁻¹ were reported at Dante in 1999 at a higher-temperature vent than the source of our sample²⁸. On the basis of these mineral equilibria, the significant increases in H₂ and H₂S at Puffer and Sully following the 1999 event indicate a shift towards a more reducing pyrite–pyrrhotite–magnetite (PPM) redox buffer (Fig. 3). The redox shift at 'A' vent was more extreme, with H₂ and H₂S levels resting solidly within the pyrrhotite stability field. These more extreme values probably result because the heat source was only 200 m below the sea floor²², and also represent incipient rock alteration by seawater-derived hydrothermal fluid²⁷. These field data are consistent with the experimentally determined redox progression of basaltic alteration by hydrothermal fluid²⁷, but increased reaction-zone temperature and decreased pressure associated with magma movement would also substantially increase H₂ and H₂S concentrations in equilibrium with basaltic rock²⁷.

Not all gases within these systems behave similarly during a magmatic event. CH₄ concentrations decreased at Endeavour in 1999, and continued to decrease at three sites in 2000 (Fig. 1h), in marked contrast to CO₂, He, H₂ and H₂S. Since 1984, anomalously high CH₄ concentrations (attributed to sedimentary involvement) have been in evidence at Endeavour²⁹. The decoupling of CH₄ concentrations from the other gases confirms that the Endeavour CH₄ source is not magmatic. CH₄ concentrations at 'A' vent, however, did show a systematic temporal trend as a result of the dyking event (Fig. 2).

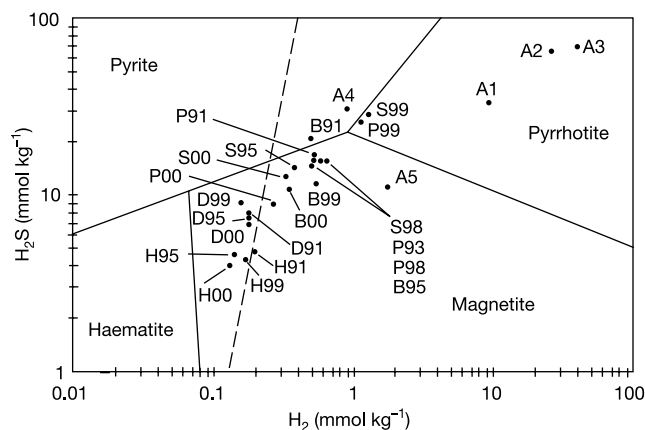


Figure 3 H₂ and H₂S concentrations plotted on the phase diagram for the mineral assemblage pyrite–pyrrhotite–magnetite (PPM) in the presence of anhydrite + anorthite–clinzoisite (dashed line). Endeavour vents are designated by H (Hulk), D (Dante), B (Bastille), P (Puffer) and S (Sully) followed by the year sampled. The mineral stability fields represent the conditions at 400 °C–500 bar, and are taken from ref. 27. These conditions are a good representation of the reaction zone at Endeavour, but the reaction zone at 'A' vent was much shallower (about 270 bar), which will shift the mineral stability fields to the right. As these low pressures promote large increases in H₂ and H₂S concentrations, the relationship of the 'A' vent samples to the stability fields is approximate.

Taking the data together—that is, the original seismic data¹³, the borehole data¹⁴, the large concentration increases in the magmatic gases CO₂ and He, and the increase in ³He/heat ratio—we conclude that the 8 June 1999 seismic swarm on Endeavour was the result of magma movement beneath the ridge crest, and not of a purely tectonic event. The data presented here confirm that magmatic events have profound effects on the characteristics of hydrothermal fluids. Magmatic activity causes transient fluxes of magmatic gases and shifts of pressure, temperature and redox conditions in the high-temperature reaction zone, thereby influencing fluid phase separation and causing large changes in the Cl concentration of hydrothermal fluids. Magmatic events can cause significant changes in the flux of ore-forming metals to the sea floor^{27,30}. The concentrations of CO₂, He and H₂ rise rapidly during magmatic events, but these concentration changes are not yet well constrained. The volatile flux during the first few months after magmatic events clearly needs to be better evaluated, as the resulting contribution of volatiles during this early period may rival that released by a mature hydrothermal system during an entire year. □

Received 2 December 2002; accepted 5 March 2003; doi:10.1038/nature01569.

1. Kelley, D. S., Baross, J. A. & Delaney, J. R. Volcanoes, fluids, and life at mid-ocean ridge spreading centers. *Annu. Rev. Earth Planet. Sci.* **30**, 385–491 (2002).
2. Delaney, J. R., Robjoug, V., McDuff, R. E. & Tivey, M. K. Geology of a vigorous hydrothermal system on the Endeavour segment, Juan de Fuca Ridge. *J. Geophys. Res.* **97**, 19663–19682 (1992).
3. Butterfield, D. A. *et al.* Gradients in the composition of hydrothermal fluids from the Endeavour segment vent field: phase separation and brine loss. *J. Geophys. Res.* **99**, 9561–9583 (1994).
4. Johnson, H. P. *et al.* Earthquake-induced changes in a hydrothermal system on the Juan de Fuca mid-ocean ridge. *Nature* **407**, 174–177 (2000).
5. Kappel, E. S. & Ryan, W. B. F. Volcanic episodicity and a non-steady state rift valley along northeast Pacific spreading centers: evidence from Sea MARC I. *J. Geophys. Res.* **91**, 13925–13940 (1986).
6. Rohr, K. M. M., Milkereit, B. & Yorath, C. J. Asymmetric deep crustal structure across the Juan de Fuca Ridge. *Geology* **16**, 533–537 (1988).
7. White, D. J. & Clowes, R. M. Shallow crustal structure beneath the Juan de Fuca Ridge from 2-D seismic refraction tomography. *Geophys. J. Int.* **100**, 349–367 (1990).
8. Wilcock, W. S. D., Archer, S. D. & Purdy, G. M. Microearthquakes on the Endeavour segment of the Juan de Fuca Ridge. *J. Geophys. Res.* **B 107**, doi:10.1029/2001JB000505 (2002).
9. Lister, C. R. B. in *Hydrothermal Processes at Seafloor Spreading Centers* (eds Rona, P. A., Boström, K., Laubier, L. & Smith, K. L. Jr) 141–168 (Plenum, New York, 1983).
10. Wilcock, W. S. D. & Delaney, J. R. Mid-ocean ridge sulfide deposits: evidence for heat extraction from magma chambers or cracking fronts? *Earth Planet. Sci. Lett.* **145**, 49–64 (1996).
11. Detrick, R. S. *et al.* New multichannel seismic constraints on the crustal structure of the Endeavour Segment, Juan de Fuca Ridge: Evidence for a crustal magma chamber. *Eos* **83**, F1353 (2002).
12. Lowell, R. P. & Germanovich, L. N. On the temporal evolution of high-temperature hydrothermal systems at ocean ridge crests. *J. Geophys. Res.* **99**, 565–575 (1994).
13. Bohnenstiehl, D. R., Tolstoy, M., Dziak, R. P., Fox, C. G. & Smith, D. K. Aftershock sequences in the mid-ocean ridge environment: an analysis using hydroacoustic data. *Tectonophysics* **354**, 49–70 (2002).
14. Davis, E. E., Wang, K., Thompson, R. E., Becker, K. & Cassidy, J. F. An episode of seafloor spreading and associated plate deformation inferred from crustal fluid pressure transients. *J. Geophys. Res.* **106**, 21953–21963 (2001).
15. Butterfield, D. A., Massoth, G. J., McDuff, R. E., Lupton, J. E. & Lilley, M. D. Geochemistry of hydrothermal fluids from Axial Seamount hydrothermal emissions study vent field, Juan de Fuca Ridge: subseafloor boiling and subsequent fluid-rock interaction. *J. Geophys. Res.* **95**, 12895–12921 (1990).
16. Sedwick, P. N., McMurtry, G. M. & MacDougall, J. D. Chemistry of hydrothermal solutions from Pele's Vents, Loihi seamount, Hawaii. *Geochim. Cosmochim. Acta* **56**, 3643–3667 (1992).
17. Lupton, J. E., Lilley, M. D., Olson, E. J. & Von Damm, K. L. Gas chemistry of vent fluids from 9°–10° N on the East Pacific Rise. *Eos* **72**, F481 (1991).
18. Lilley, M. D., Olson, E. J., McLaughlin, E. & Von Damm, K. L. Methane, hydrogen and carbon dioxide in vent fluids from the 9°N hydrothermal system. *Eos* **72**, F481 (1991).
19. Dixon, J. E., Stolper, E. M. & Holloway, J. R. An experimental study of water and carbon dioxide solubilities in mid-ocean ridge basaltic liquids. Part I: Calibration and solubility models. *J. Petrol.* **36**, 1607–1631 (1995).
20. Dixon, J. E., Stolper, E. & Delaney, J. R. Infrared spectroscopic measurements of CO₂ and H₂O in Juan de Fuca Ridge basaltic glasses. *Earth Planet. Sci. Lett.* **90**, 87–104 (1988).
21. Kadko, D. & Butterfield, D. A. The relationship of hydrothermal fluid composition and crustal residence time to maturity of vent fields on the Juan de Fuca Ridge. *Geochim. Cosmochim. Acta* **62**, 1521–1533 (1998).
22. Stuart, F. M. & Turner, G. Mantle-derived ⁴⁰Ar in mid-ocean ridge hydrothermal fluids: implications for the source of volatile and mantle degassing rates. *Chem. Geol.* **147**, 77–88 (1998).
23. Seewald, J. S., Cruse, A. M. & Saccocia, P. J. Aqueous volatiles in hydrothermal fluids from the Main Endeavour vent field: Temporal variability following earthquake activity. *Eos* **82**, F615 (2001).
24. Von Damm, K. L. *et al.* Evolution of East Pacific Rise hydrothermal vent fluids following a volcanic eruption. *Nature* **375**, 47–50 (1995).
25. Sohn, R. A., Fornari, D. J., Von Damm, K. L., Hildebrand, J. A. & Webb, S. C. Seismic and hydrothermal evidence for a cracking event on the East Pacific Rise crest at 9° 50' N. *Nature* **396**, 159–161 (1998).
26. Lupton, J. E., Baker, E. T. & Massoth, G. J. Helium, heat, and the generation of hydrothermal event plumes at mid-ocean ridges. *Earth Planet. Sci. Lett.* **171**, 343–350 (1999).

27. Seyfried, W. E. Jr & Ding, K. *Seafloor Hydrothermal Systems: Physical, Chemical, Biological and Geological Interactions* (eds Humphris, S. E., Zierenberg, R. A., Mullineaux, L. S. & Thomson, R. E.) 248–272 (American Geophysical Union, Washington DC, 1995).
28. Ding, K., Seyfried, W. E. Jr, Tivey, M. K. & Bradley, A. M. In situ measurement of dissolved H₂ and H₂S in high-temperature hydrothermal vent fluids at the Main Endeavour Field, Juan de Fuca Ridge. *Earth Planet. Sci. Lett.* **186**, 417–425 (2001).
29. Lilley, M. D. *et al.* Anomalous CH₄ and NH₄⁺ concentrations at an unsedimented mid-ocean-ridge hydrothermal system. *Nature* **364**, 45–47 (1993).
30. Von Damm, K. L. Chemistry of hydrothermal vent fluids from 9° - 10° N, East Pacific Rise: "Time zero," the immediate post-eruptive period. *J. Geophys. Res.* **105**, 11203–11222 (2000).

Supplementary Information accompanies the paper on Nature's website (http://www.nature.com/nature).

Acknowledgements We thank L. Evans and K. Roe for technical assistance, D. Kelley for a critical reading of the manuscript, W. Wilcock for discussions, and W. E. Seyfried Jr for the opportunity to join his 1999 cruise to Endeavour. The manuscript was improved by comments and suggestions from J. Seewald and R. Lowell. This work was supported by the National Science Foundation and in part by the National Oceanic and Atmospheric Administration VENTS Program.

Competing interests statement The authors declare that they have no competing financial interests.

Correspondence and requests for materials should be addressed to M.D.L. (e-mail: lilley@ocean.washington.edu).

A test of the unified neutral theory of biodiversity

Brian J. McGill

Department of Ecology and Evolutionary Biology, University of Arizona, Tucson, Arizona 85721, USA

One of the fundamental questions of ecology is what controls biodiversity. Recent theory suggests that biodiversity is controlled predominantly by neutral drift of species abundances^{1–4}. This theory has generated considerable controversy^{5–12}, because it claims that many mechanisms that have long been studied by ecologists (such as niches) have little involvement in structuring communities. The theory predicts that the species abundance distribution within a community should follow a zero-sum multinomial distribution (ZSM), but this has not, so far, been rigorously tested. Specifically, it remains to be shown that the ZSM fits the data significantly better than reasonable null models. Here I test whether the ZSM fits several empirical data sets better than the lognormal distribution. It does not. Not only does the ZSM fail to fit empirical data better than the lognormal distribution 95% of the time, it also fails to fit empirical data better even a majority of the time. This means that there is no evidence that the ZSM predicts abundances better than the much more parsimonious null hypothesis.

The unified neutral theory of biodiversity (or UNTB, hereafter used to refer to either the theory or Hubbell's 2001 book¹) predicts that species abundance distributions (SADs) should follow the ZSM (see Box 1). To test whether the ZSM fits the data better than the null lognormal hypothesis, I used two data sets. First, I used the North American Breeding Bird Survey^{13–15} (BBS), for the simple reason that it is one of the few data sets that has replicates (in this case different sites) taken with identical sampling methodologies. Replicates are important for testing statistical significance. Since the ZSM has been applied primarily to intensively sampled data, I averaged the BBS data over a five-year period (1996–2000). Thus, rare species that show up only once in five years are included. I took 100 replicates by randomly selecting 100 routes that were rated to be of high quality for all five years. As an alternative data source, I also used the well-known Barro Colorado Island (BCI) tree data set, in